

Preclinical Strategies to Identify Off-Target Toxicity of High-Affinity TCRs

Helena M. Bijen,¹ Dirk M. van der Steen,¹ Renate S. Hagedoorn,¹ Anne K. Wouters,¹ Linda Wooldridge,² J.H. Frederik Falkenburg,¹ and Mirjam H.M. Heemskerk¹

¹Department of Hematology, Leiden University Medical Center, Leiden, the Netherlands; ²Faculty of Health Sciences, University of Bristol, Biomedical Sciences Building, Bristol, UK

Adoptive transfer of T cells engineered with a cancer-specific T cell receptor (TCR) has demonstrated clinical benefit. However, the risk for off-target toxicity of TCRs remains a concern. Here, we examined the cross-reactive profile of T cell clone (7B5) with a high functional sensitivity for the hematopoietic-restricted minor histocompatibility antigen HA-2 in the context of HLA-A*02:01. HA-2^{Pos} Epstein-Barr virus-transformed B lymphoblastic cell lines (EBV-LCLs) and primary acute myeloid leukemia samples, but not hematopoietic HA-2^{neg} samples, are effectively recognized. However, we found unexpected off-target recognition of human fibroblasts and keratinocytes not expressing the HA-2 antigen. To uncover the origin of this off-target recognition, we performed an alanine scanning approach, identifying six out of nine positions to be important for peptide recognition. This indicates a low risk for broad cross-reactivity. However, using a combinatorial peptide library scanning approach, we identified a *CDH13*-derived peptide activating the 7B5 T cell clone. This was confirmed by recognition of *CDH13*-transduced EBV-LCLs and cell subsets endogenously expressing *CDH13*, such as proximal tubular epithelial cells. As such, we recommend the use of a combinatorial peptide library scan followed by screening against additional cell subsets to validate TCR specificity and detect off-target toxicity due to cross-reactivity directed against unrelated peptides before selecting candidate TCRs for clinical testing.

INTRODUCTION

Immunotherapy has obtained a prominent role in the field of oncology and has proven valuable in the treatment of different types of tumors. A range of immunotherapies are under development, varying from chimeric antigen receptors (CARs),¹ expanding tumor-infiltrating lymphocytes (TILs)^{2,3} and T cell receptor (TCR)-transduced effector cells.^{4,5} Various studies successfully make use of TCR-engineered T cells to enhance patients' adaptive immune responses against malignancies, demonstrating potent anti-tumor reactivity.⁶⁻⁹

No matter how promising therapies using TCR-engineered T cells may be, they come with side effects and risks. T cells are naturally checked for recognition of self-peptides in the context of self-human leukocyte antigen (HLA) and deleted in the thymus if this recognition is too strong, in a process called negative selection.¹⁰ This selection

process is absent or non-optimal when TCRs are derived from donors with mismatched HLA typing, when they are isolated from humanized mouse models expressing only one HLA molecule and no human proteins, or when TCRs are structurally altered for affinity enhancement.^{11,12}

Affinity enhancement of TCRs can result in both on- and off-target toxicity.¹³ Recent examples of clinically tested TCRs directed against MAGE-A3 and MART-1 demonstrated severe toxicities.^{12,14-17} In the clinical trial testing a modified anti-MAGE-A3 TCR, derived from immunization of HLA-A*02:01 transgenic mice, two out of nine cancer patients developed fatal on-target neurological toxicity, due to recognition of a peptide derived from the same gene family that is expressed in the brain.¹⁵ In another trial, where an affinity-enhanced anti-MAGE-A3 TCR was tested in myeloma and melanoma patients, two patients died of off-target toxicity caused by recognition of a completely different peptide, resulting in severe myocardial damage.^{12,17} These clinical cases show how difficult it is to predict the exact specificity and the resulting effects of TCRs that did not undergo optimal thymic selection. It is crucial to develop strategies to extensively validate the exact specificity of TCRs, particularly because TCR-engineered T cells are highly sensitive.^{14,18}

In this study, we aimed to develop a reliable screening pipeline for early detection of off-target toxicity due to the cross-reactivity of TCRs directed against unrelated peptides. In previous work, we have focused on the identification of therapeutic TCRs directed against hematopoietic restricted minor histocompatibility antigens (MiHAs) for the treatment of hematological malignancies. The HLA-A*02:01 restricted HA-2 peptide YIGEVLVSV is a well-known example of such an MiHA.^{19,20} In recent experiments we isolated an HA-2-specific T cell clone, 7B5, using an *in vitro* HLA-mismatched setting. We validated its specificity for the HA-2 antigen in hematopoietic cell subsets. However, we found unexpected off-target recognition of human fibroblasts not expressing the HA-2 antigen,

Received 1 November 2017; accepted 16 February 2018;
<https://doi.org/10.1016/j.ymthe.2018.02.017>.

Correspondence: Mirjam H.M. Heemskerk, Department of Hematology, Leiden University Medical Center, C2-R, P.O. Box 9600, 2300 RC Leiden, the Netherlands.
E-mail: m.h.m.heemskerk@lumc.nl



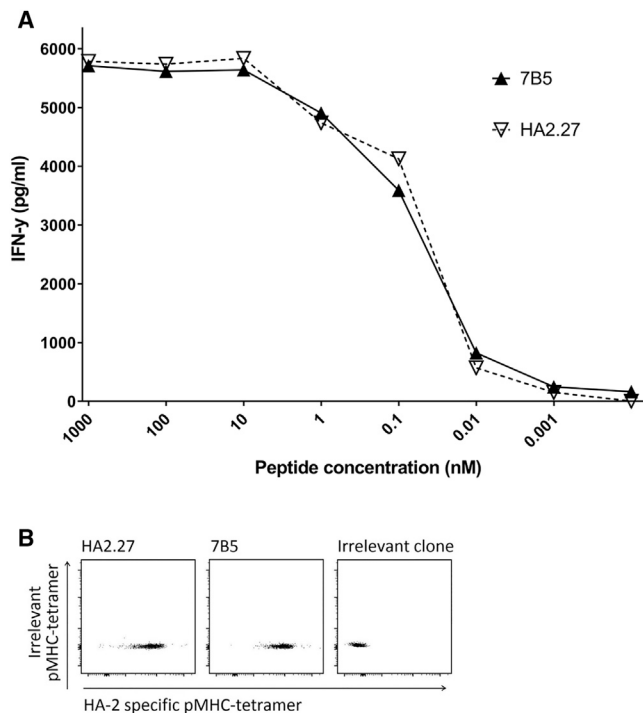


Figure 1. The 7B5 T Cell Clone Exhibits Similar Sensitivity to HA-2 Compared with Clone HA2.27 in a Peptide Stimulation Assay and pMHC-Tetramer Staining

(A) T cell clones 7B5 and HA2.27 (5,000/well) were cocultured with T2 cells (30,000/well) loaded with HA-2 peptide at different concentrations. After overnight incubation, supernatants were harvested, and the concentration of IFN- γ was measured by ELISA. (B) T cell clones were analyzed for binding to specific APC-labeled pMHC-tetramers. Depicted dot plots are gated for CD8^{pos} lymphocytes.

raising the questions what triggered this activation and what method is suitable to examine this. Thus, we investigated the off-target cross-reactive potential of this high-avidity T cell clone using different screening methods and characterized its fine specificity.

Currently, an amino acid scanning approach is the recommended method,²¹ which we compared with screening with a 9-mer combinatorial peptide library (CPL).²² To validate recognition of predicted cross-reactive target peptides by the 7B5 T cell clone, as discovered by the different screening approaches, we then screened the 7B5 T cell clone against several non-hematopoietic cell subsets endogenously expressing these peptides. As a control, we used an HA-2-specific T cell clone, HA2.27, previously isolated from a chronic myeloid leukemia patient who experienced a graft-versus-leukemia (GvL) response after HLA-matched stem cell transplantation (SCT) and subsequent donor lymphocyte infusion (DLI).²³ The patient from whom these clones were isolated did not experience any harmful GvHD,²⁴ and no *ex vivo* cross-reactivity was discovered.

We show that the amino acid scanning approach alone provided useful information about which amino acid positions in the peptide

are important for TCR recognition, but its ability to elucidate the cross-reactivity profile of the 7B5 TCR was limited. Instead, we were able to detect off-target reactivity directed against a peptide derived from *CDH13* using a CPL scanning approach. This was confirmed with *CDH13*-transduced HA-2^{neg} Epstein-Barr virus-transformed B lymphoblastic cell lines (EBV-LCLs), and the potential *in vivo* consequences were deduced by screening against a broad range of different cell subsets.

RESULTS

Identification of an HA-2-Specific T Cell Clone from the Allogeneic TCR Repertoire

T cell clones from an HLA-A*02:01^{neg} individual were isolated using peptide-major histocompatibility complex (pMHC)-tetramers composed of the HA-2 peptide bound to HLA-A*02:01. pMHC-tetramer^{pos} cells were first enriched by magnetic-activated cell sorting (MACS) followed by single-cell sorting of pMHC-tetramer^{pos} CD8^{pos} T cells. T cell clones were selected that demonstrated reactivity against T2 cells loaded with the HA-2 peptide, but not against unloaded T2 cells. Among these T cell clones, clone 7B5 demonstrated the highest functional sensitivity when stimulated with titrated amounts of HA-2 peptide. This reactivity was comparable with the patient-derived control clone HA2.27, which was isolated from a beneficial GvL response after allogeneic SCT and subsequent DLI (Figure 1A).

Specific binding to the allophycocyanin (APC)-labeled HA-2 pMHC-tetramer was validated for both T cell clones. Both the 7B5 T cell clone and the HA2.27 T cell clone showed specific staining with the APC-labeled HA-2 pMHC-tetramer with similar intensity (Figure 1B).

Expression of the *MYO1G* gene, encoding for the MiHA HA-2, is restricted to hematopoietic tissues.²⁰ We confirmed this restricted expression in an in-house-generated microarray gene expression database (Figure S1).²⁵ To investigate whether T cell clone 7B5 was able to selectively recognize cell subsets expressing HA-2, we tested the HA-2 reactive T cell clones against different hematopoietic cell subsets, starting with SNP-genotyped EBV-LCLs that were either positive or negative for the MiHA HA-2. Robust recognition of HLA-A*02:01^{pos} HA-2^{pos} EBV-LCLs, but not HLA-A*02:01^{pos} HA-2^{neg} or HLA-A*02:01^{neg} EBV-LCLs, was detected, which was comparable with the HA2.27 T cell clone (Figure 2A). In addition, the anti-tumor reactivity of T cell clone 7B5 was tested against different HLA-A*02:01^{pos} primary acute myeloid leukemia (AML) samples either positive or negative for the MiHA HA-2. HLA-A*02:01^{pos} fibroblasts and HLA-A*02:01^{pos} keratinocytes were included as HA-2^{neg} controls. HA-2^{pos} AML samples were similarly recognized by both the HA2.27 T cell clone and the 7B5 T cell clone, whereas the HA-2^{neg} AML sample was not (Figure 2B). However, the HLA-A*02:01^{pos} HA-2^{neg} fibroblasts and keratinocytes that were not recognized by the HA2.27 T cell clone as expected were efficiently recognized by the 7B5 T cell clone (Figure 2B).

All these results indicate that the 7B5 T cell clone is a high-avidity T cell clone, capable of targeting HA-2-expressing hematopoietic

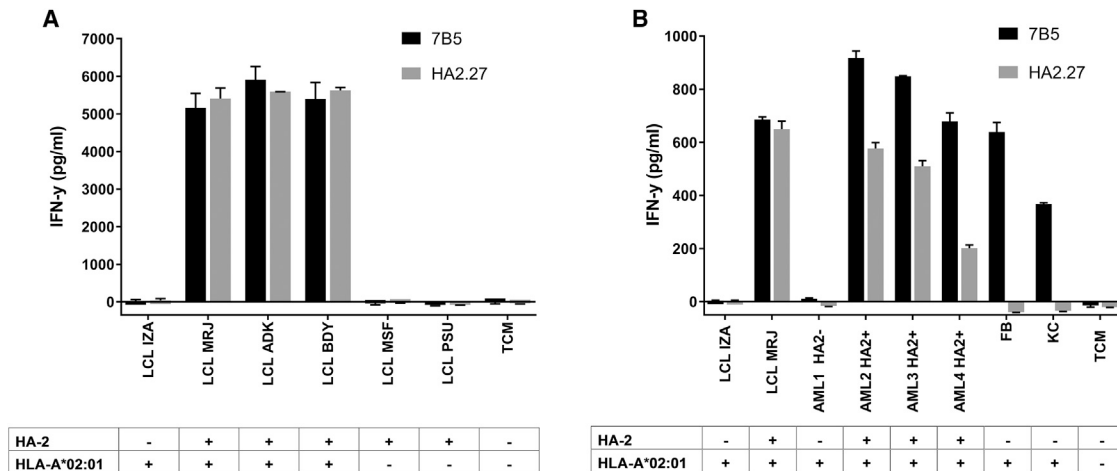


Figure 2. The 7B5 T Cell Clone Recognizes HA-2-Expressing EBV-LCLs and Primary AML Samples

(A) T cell clones 7B5 and HA2.27 (5,000/well) were cocultured with several EBV-LCLs at a stimulator-to-responder (S:R) ratio of 6:1. Controls included EBV-LCLs from the patient (LCL MRJ, HLA-A*02:01^{pos} HA-2^{pos}) and donor (LCL IZA, HLA-A*02:01^{pos} HA-2^{neg}) we isolated T cell clone HA2.27 from, as well as HLA-A*02:01^{neg} controls LCL-MSF and LCL-PSU. After overnight incubation, supernatants were harvested, and the concentration of IFN- γ was measured by ELISA. Depicted values are the average of duplicate measurements \pm SD. (B) T cell clones 7B5 and HA2.27 (5,000/well) were cocultured with HLA-A*02:01^{pos} HA-2^{neg} primary AML sample (AML1), HLA-A*02:01^{pos} HA-2^{pos} primary AML samples (AML2,-3,-4), and HLA-A*02:01^{pos} HA-2^{neg} fibroblasts (FB) and keratinocytes (KC) at an S:R ratio of 6:1. After overnight incubation, supernatants were harvested, and the concentration of IFN- γ was measured by ELISA. Depicted values are the average of duplicate measurements \pm SD.

cell subsets in the context of HLA-A*02:01. Unexpectedly, the 7B5 T cell clone recognized HLA-A*02:01^{pos} HA-2^{neg} human fibroblasts and keratinocytes as well.

Analysis of Off-Target Cross-Reactivity of the 7B5 T Cell Clone

We showed that the 7B5 T cell clone and the HA2.27 T cell clone have a similar functional sensitivity for HA-2, but the 7B5 T cell clone demonstrated cross-reactivity against HA-2^{neg} fibroblasts and keratinocytes. In order to assess what causes this off-target recognition of fibroblasts and keratinocytes, we used an alanine scanning approach. Both HA-2-reactive clones were tested against the immunogenic HA-2 sequence (YIGEVLVSV), the naturally occurring non-immunogenic counterpart (YIGEVLVSM), and newly synthesized HA-2 peptides in which every amino acid is sequentially replaced by an alanine (A). In Table 1 the different peptides are summarized. According to NetMHC4.0, none of the alanine substitutions interfere with HLA-A*02:01 binding to a relevant extent. Both HA-2 T cell clones were incubated overnight with peptide-pulsed T2 cells at different concentrations (8, 40, and 200 nM), and IFN- γ production was measured. When alanine substitution resulted in a substantial decrease in IFN- γ production compared with the immunogenic HA-2 sequence, this position was considered essential. The results, depicted in Figures 3A–3C, demonstrate that for T cell clone 7B5, positions 2, 3, 4, 5, 6, and 7 were important for HA-2-specific recognition. This recognition pattern was slightly different from the HA-2.27 clone, because for this clone, positions 1, 2, 3, 4, and 6 were important for HA-2-specific recognition.

For the 7B5 T cell clone, an *in silico* search was carried out to identify protein sequences that contain the motif X-I-G-E-V-L-V-X-X. We

searched for human self-protein-derived peptide sequences with this motif using the ScanProsite webtool. Besides the HA-2 peptide, this search resulted in only one other peptide sequence PIGEVLVSS derived from the human gene KLF6. However, this KLF6-derived sequence was not predicted to bind HLA-A*02:01 according to NetMHC4.0; thus, we concluded that there was a low risk of cross-reactivity, based on this amino acid scanning approach.

Next, we performed a 9-mer CPL scan. This CPL is composed of 180 different 9-mer peptide mixtures. In every peptide mixture one amino acid position has a fixed L-amino acid residue, but all other positions are degenerate, enabling incorporation of any 1 of 19 natural L-amino acids in all remaining 8 positions (cysteine is excluded). The 7B5 T cell clone was incubated overnight with T2 cells pulsed with the 180 different peptide mixtures, and IFN- γ production was measured. Results are depicted in a heatmap (Figure 4). Using the WSBC PI CPL webtool, we conducted a 9-mer CPL-driven search of the human self-protein database to produce a list of the top 100 peptide sequences ranked in order of likelihood of recognition (Table S1). After removing duplicate sequences, a list of 42 peptide sequences remained and were further refined on the basis of whether they were predicted to bind HLA-A*02:01 using NetMHC4.0. This resulted in a final list of 10 peptide sequences, which were subsequently synthesized (Table 2). The ability of the T cell clones 7B5 and HA2.27 to recognize these candidate peptides was determined by measuring the IFN- γ production after stimulation with T2 cells loaded with titrated concentrations of these peptides. Only one peptide, the CDH13-derived peptide (p01) SVGSVLLTV, was recognized with a similar sensitivity as the HA-2 peptide (p02) (Figure 5A). The patient-derived HA2.27 control clone did not recognize any other peptide but HA-2 (Figure 5B).

Table 1. HLA-A*02:01 Binding Properties of the Peptides Used for the Amino Acid Scanning Approach

Sequence	netMHC4.0 (nM); Binding Level
YIGEVLVSV	7.0; SB
YIGEVLVSM	57.7; WB
AIGEVLVSV	33.4; SB
YAGEVLVSV	41.6; WB
YIAEVLVSV	3.3; SB
YIGAVLVSV	12.9; SB
YIGEALVSV	7.6; SB
YIGEVAVSV	14.9; SB
YIGEVLASV	7.1; SB
YIGEVLVAV	9.1; SB
YIGEVLVSA	30.6; SB

WB, weak binder; SB, strong binder.

In order to confirm processing and presentation of the *CDH13*-derived peptide in HLA-A*02:01, we transduced *CDH13* into two different HLA-A*02:01^{Pos} HA-2^{neg} EBV-LCLs (IZA and HRK). Recognition of the transduced and untransduced EBV-LCLs was evaluated by IFN- γ ELISA. The 7B5 T cell clone did not recognize untransduced HLA-A*02:01^{Pos} HA-2^{neg} EBV-LCLs, similar to the HA2.27 T cell clone, but *CDH13* transduced HLA-A*02:01^{Pos} HA-2^{neg} EBV-LCLs were highly recognized by the 7B5 T cell clone, whereas the HA2.27 T cell clone was not able to recognize these transduced EBV-LCLs (Figure 5C). These results demonstrate that T cell clone 7B5 is cross-reactive against the *CDH13*-derived peptide.

Cross-Reactivity Directed against *CDH13*

We showed that T cell clone 7B5 is cross-reactive toward a *CDH13*-derived peptide, which is presented by HLA-A*02:01. Next, we wanted to investigate the possible implications of this cross-reactivity *in vivo*. According to our gene expression microarray database,²⁵ the *CDH13* gene is expressed by a wide variety of healthy non-hematopoietic cell subsets, e.g., fibroblasts, keratinocytes, proximal tubular epithelial cells, and the melanoma cell line FM6 (Figure S2). We tested the 7B5 T cell clone against keratinocytes and fibroblasts derived from HLA-A*02:01^{Pos} donors, either untreated or pretreated with IFN- γ for 2 days to upregulate HLA expression, and HLA-A*02:01^{Pos} proximal tubular epithelial cells and melanoma cell line FM6. All cell subsets were recognized by the 7B5 T cell clone, but not by the HA2.27 T cell clone (Figure 6). To confirm that only HLA-A*02:01-restricted epitopes were recognized, we included HLA-A*02:01^{neg} fibroblasts, either untreated or pretreated with IFN- γ for 2 days. The HLA-A*02:01^{neg} fibroblasts were unable to activate the 7B5 T cell clone (Figure 6).

All these results demonstrate that the 7B5 T cell clone can activate in response to both the HA-2 antigen and the *CDH13*-derived peptide

SVGSVLLTV, causing cross-reactivity restricted to HLA-A*02:01^{Pos} tissues.

DISCUSSION

In this study, we detected off-target reactivity of the 7B5 TCR directed against a peptide derived from the gene *CDH13* using a CPL scanning approach, which was confirmed by the ability of the 7B5 T cell clone to recognize *CDH13*-transduced HA-2^{neg} EBV-LCLs and several cell subsets endogenously expressing *CDH13*. We show that the standard alanine scanning approach alone provided useful information about which amino acid positions in the peptide are important for TCR recognition, but its ability to elucidate cross-reactivity for the 7B5 TCR was limited.

The 7B5 T cell clone was isolated from an HLA-A*02:01-negative donor; thus, because of the HLA-mismatched experimental setting, thymic selection did not occur. The 7B5 T cell clone recognizes the hematopoietic restricted MiHA HA-2 in the context of HLA-A*02:01. The 7B5 T cell clone was shown to have a functional sensitivity that was similar to the patient-derived T cell clone HA2.27, because concentrations less than 1 nM HA-2 peptide loaded on T2 cells could still trigger IFN- γ production. Also, endogenously processed and presented HA-2 peptide was effectively recognized by the 7B5 T cell clone, as indicated by IFN- γ production upon incubation with HA-2^{Pos} EBV-LCLs and primary AML samples. Results were similar to the HA2.27 T cell clone, and no recognition of HA-2^{neg} EBV-LCLs or primary AML samples was observed.

The results of the alanine scanning approach suggested a low risk for broad cross-reactivity of the 7B5 T cell clone, because exchanging the amino acid for an alanine at positions 2, 3, 4, 5, 6, or 7 resulted in complete loss of peptide recognition. These results do not exclude the possibility of cross-reactivity toward other specific peptides, but it dismisses the risk of a highly promiscuous TCR. A search for specific human self-protein-derived peptides with the motif X-I-G-E-V-L-V-X-X did not yield any potential off-target toxicity candidates. However, when we used the 9-mer CPL scan data to conduct a CPL-driven search of the human self-protein database, we found cross-reactivity directed against a peptide derived from the gene *CDH13*. This was confirmed by the ability of the 7B5 T cell clone to recognize HA-2^{neg} EBV-LCLs transduced with the *CDH13* gene and a range of tissues that endogenously express *CDH13* including fibroblasts, keratinocytes, and proximal tubular epithelial cells (PTECs).

All of these results demonstrate that the 7B5 T cell clone can activate in response to healthy HLA-A*02:01^{Pos} tissues such as fibroblasts, which is likely to have severe clinical consequences if this TCR was engineered into T cells for adoptive therapy in patients. Therefore, we conclude that thorough validation of the specificity and characterization of cross-reactivity by combining several screening techniques should be a strict prerequisite for TCRs to be tested prior to their use in the clinic.

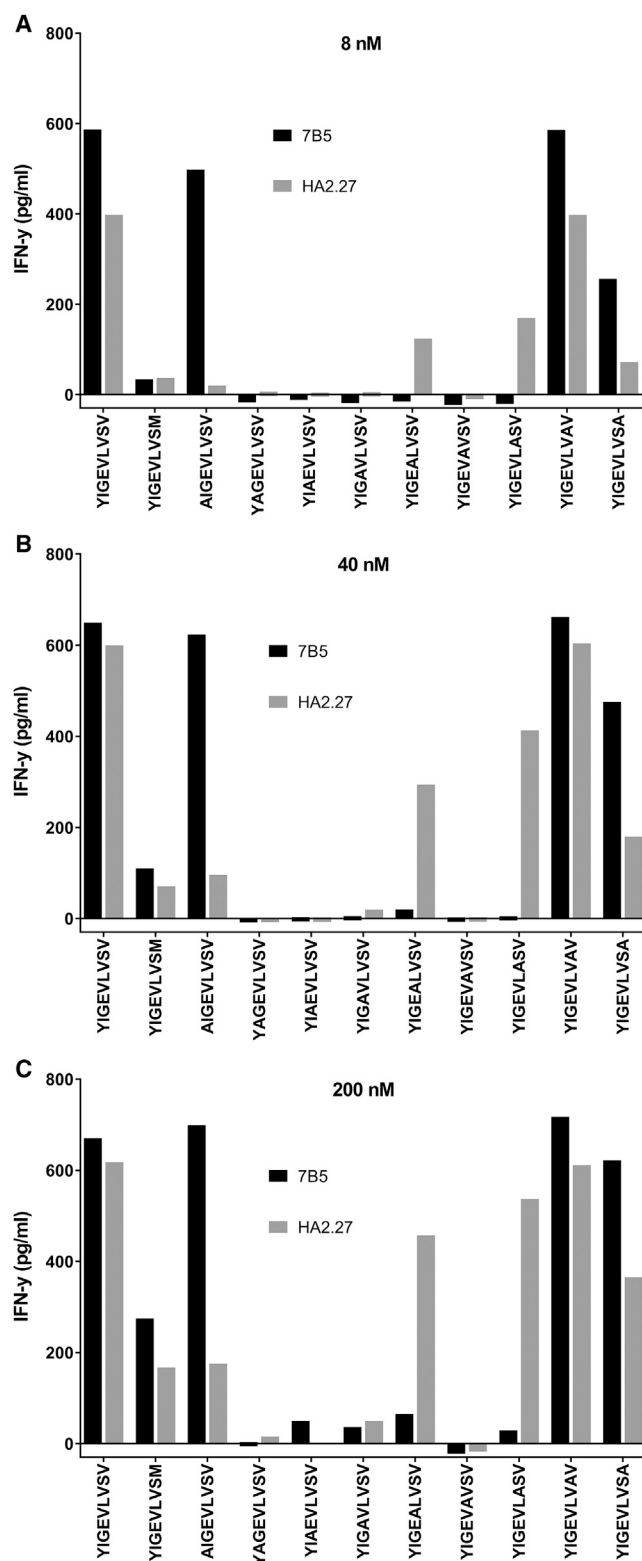


Figure 3. The Alanine Scanning Approach for T Cell Clones 7B5 and HA2.27 T cell clones 7B5 and HA2.27 (5,000/well) were cocultured with T2 cells (30,000/well), loaded with 8 (A), 40 (B), and 200 nM (C) peptides. After overnight incubation,

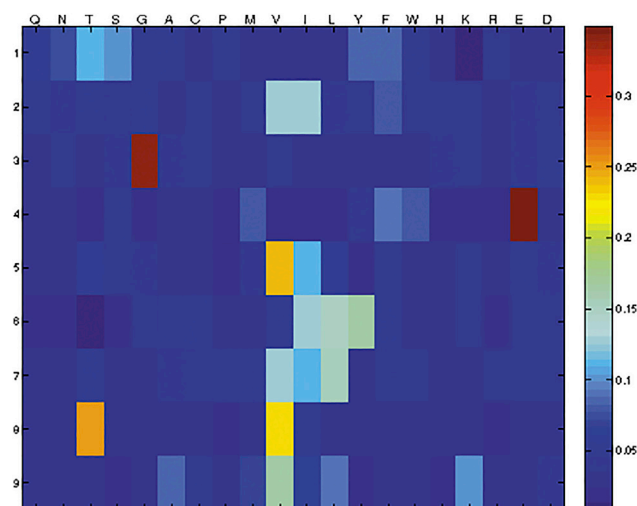


Figure 4. A Heatmap Representation of a 9-Mer CPL Scan of the 7B5 T Cell Clone

A heatmap depicting the intensity of IFN- γ production by the 7B5 T cell clone (4,000/well) in response to T2 cells (20,000/well) loaded with the 180-peptide mixtures in a 9-mer CPL scan, indicating which amino acids are preferentially recognized at certain positions in the peptide sequence. CPL scan data are normalized in each row so that the values range from high (red) to low (blue); the maximum intensity is the largest of all red values in the rows. Amino acids are grouped according to their physicochemical properties as follows: polar, uncharged amines: Q, N; polar, uncharged alcohols: T, S; small: G, A, C; hydrophobic: A-H; aliphatic: V, I, L; aromatic: Y, F, W, H; large: F, W; charged basic: H, K, R; and charged acidic: E, D.

The alanine scanning approach was insufficient for detecting potentially dangerous cross-reactivities, whereas a CPL-driven search of the human self-protein database enabled the identification of a potentially dangerous reactivity directed toward a human self-protein-derived epitope. In the alanine scanning approach, only one amino acid is replaced at a time and the amino acids are only replaced with a single amino acid (alanine), and not with other amino acids possessing different properties. So it is no surprise that cross-reactivity against a peptide that differs from the MiHA peptide HA-2 in five amino acid positions cannot be discovered using this assay. Because the 9-mer CPL fixes only one amino acid at one position per peptide mixture, all possible sequences (except those with more than one cysteine) are represented in the assay, and cross-reactive peptides that differ substantially from the immunogenic target peptide can be identified. The downside of this approach is that every mixture consists of many peptides, lowering the concentration per unique peptide and increasing the competition for HLA binding within every mixture. These factors might influence the results and could explain why for some T cell

IFN- γ concentrations were measured in the supernatant by ELISA. Where alanine substitution resulted in a substantial decrease in IFN- γ production compared with the immunogenic HA-2 sequence, the residue at this position was considered essential.

Table 2. Selected Potential Cross-Reactive Human Self-Protein-Derived Peptide Targets of the 7B5 T Cell Clone

Peptide No.	Peptide Sequence	Amino Acid Difference	netMHC4.0 (nM; Binding Level)	Gene	Protein Accession No. (NCBI)
p01	SVGSVLLTV	5	160.5; WB	<i>CDH13</i>	NP_001207417
p02	YIGEVLSV	–	7.0; SB	<i>MYO1G</i>	NP_149043
p03	FVGEDLVTI	5	42.6; WB	<i>BACE2</i>	NP_036237
p04	YIGENILVL	5	48.7; WB	<i>ASIC1</i>	NP_001086
p05	TLQEVLLTV	5	11.8; SB	<i>GZMH</i>	NP_219491
p06	FIGEVVSV	2	8.1; SB	<i>MYO1D</i>	NP_056009
p07	SVGEVLQSV	3	116.2; WB	<i>AKAP3</i>	NP_006413
p08	YIGQVLVTA	3	253.2; WB	<i>EML5</i>	NP_899243
p09	AQGEVQLTV	5	144.1; WB	<i>PLXNB2</i>	NP_036533
p10	TLGNVLVTV	4	26.7; SB	<i>EXOC1</i>	NP_001020095

The peptides in this table are selected based on their predicted recognition by the 7B5 TCR according to a CPL-driven search of the human self-protein database conducted using the WSBC PI CPL webtool, and subsequently filtered based on their ability to bind HLA-A*02:01 as predicted by NetMHC4.0. Peptides are ordered based on their predicted likelihood of recognition. WB, weak binder; SB, strong binder.

clones that we tested with the 9-mer CPL, a sufficient peptide recognition signature could not be determined (data not shown). Also, the 9-mer CPL-driven search of the human self-protein database produces such a great number of potential candidates that a selection strategy is needed to keep further screening experiments manageable, risking unwanted exclusion of the target peptides you are searching for.

Although the 7B5 T cell clone, which is derived from an HLA-mismatched setting, showed a potentially dangerous cross-reactivity, this does not mean that all TCRs from an allogeneic setting are of lesser clinical interest compared with clones derived from HLA-matched settings, e.g., the patient-derived T cell clone HA2.27. All TCRs have an intrinsic cross-reactive capacity,²⁶ which is necessary to cover all naturally occurring antigens that may be encountered.²⁷ Thus, the relevant question is not whether a TCR is cross-reactive, but how to predict the clinical consequences of this cross-reactivity.²⁸ Therefore, thorough screening for off-target toxicity must be included in the preclinical phases, to determine whether a TCR is safe for clinical application via adoptive transfer of TCR-engineered T cells. To further reduce potential risks, the use of a so-called suicide switch could also be considered,²⁹ which enables immediate elimination of the transfused T cells upon signs of toxicity.

In summary, we demonstrate that a standard alanine scanning approach provided useful information about which positions in the peptide sequence are important for TCR recognition, but it did not predict off-target reactivity of the 7B5 TCR. However, we were able to detect off-target reactivity directed against a peptide derived from *CDH13* using a CPL-driven search of the human self-protein database, which was confirmed using *CDH13*-transduced HA-2^{neg} EBV-LCLs and screening against several different cell subsets that endogenously express *CDH13*. This example demonstrates the advantage and need of combining several screening techniques to characterize the cross-reactivity and specificity of TCRs.

MATERIALS AND METHODS

Culture Conditions and Cells

All studies using human material were approved by the Leiden University Medical Center ethical review board. Peripheral blood was obtained from healthy individuals or patients after informed consent. Peripheral blood mononuclear cells (PBMCs) were isolated using Ficoll gradient centrifugation.

T cells were cultured in T cell medium consisting of Iscove's modified Dulbecco's medium (IMDM) (Lonza) supplemented with 100 IU/mL IL-2 (Proleukin; Novartis Pharma), 5% fetal bovine serum (FBS; GIBCO, Life Technologies), 5% human serum, 2 mM L-glutamine (Lonza), and 1% penicillin/streptomycin (Lonza). T cells were stimulated using irradiated feeders in a 1:5 ratio in T cell medium supplemented with 0.8 µg/mL phytohemagglutinin (PHA; Biochrom AG) 8–16 days prior to experiments.

EBV-LCLs were generated using standard procedures and cultured in IMDM supplemented with 10% FBS, 2 mM L-glutamine, and 1% penicillin/streptomycin.

Primary AML samples from patients at time of diagnosis were thawed and cultured overnight in IMDM supplemented with 10% fetal calf serum (FCS) before use in experiments.

Fibroblasts, keratinocytes, and other non-hematopoietic cell subsets were cultured either in the absence or presence of 200 IU/mL IFN-γ for 2 days and washed twice before use in experiments.

Isolation of the HA-2-Reactive T Cell Clone 7B5

To isolate HA-2-reactive T cell clones, we incubated 500 × 10⁶ PBMCs from an HLA-A*02:01^{neg} healthy donor with phycoerythrin (PE)-labeled pMHC-tetramers, composed of HA-2 9-mer peptide (YIGEVLSV) bound in HLA-A*02:01, for 1 hr at 4°C.

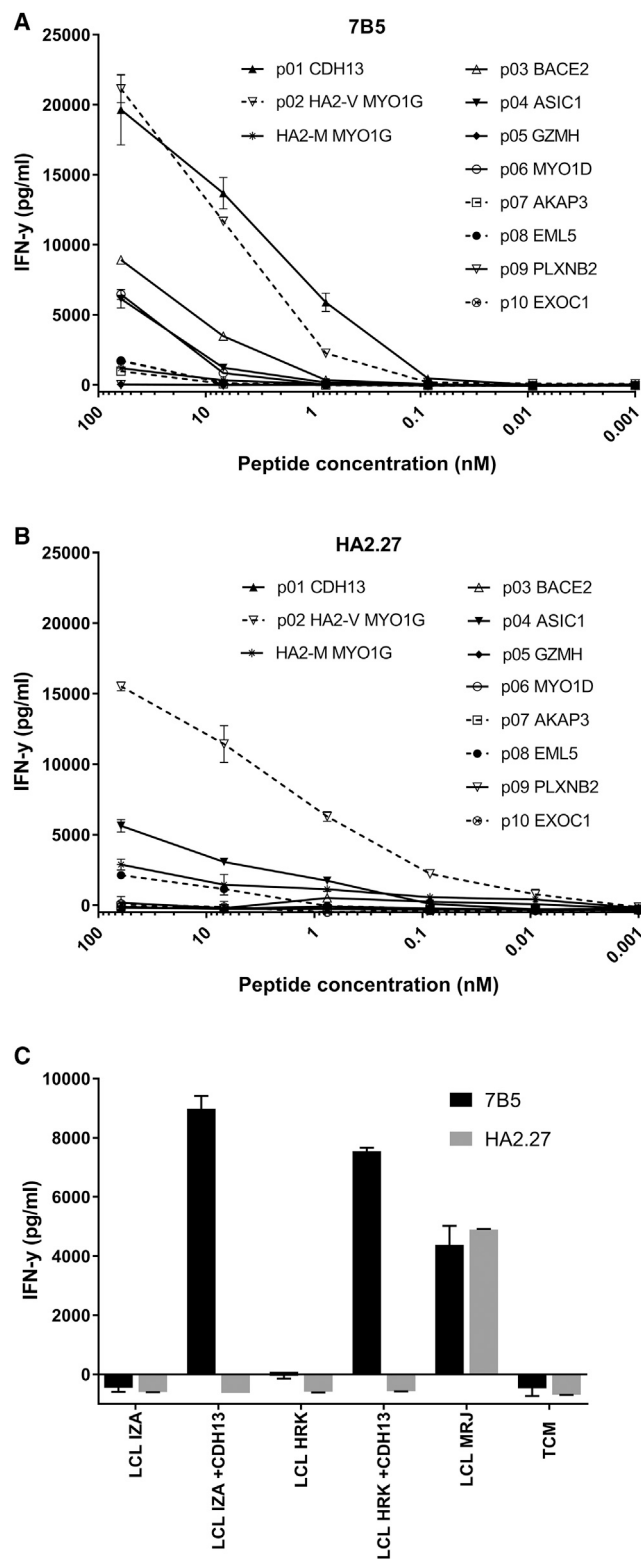


Figure 5. The 7B5 T Cell Clone Recognizes the CDH13-Derived Peptide p01, Whereas T Cell Clone HA2.27 Does Not

T cell clones (A) 7B5 and (B) HA2.27 (5,000/well) were cocultured with T2 cells (30,000) loaded with the selected peptides at different concentrations. After overnight incubation, supernatants were harvested, and the concentration of IFN- γ was measured by ELISA. Depicted values are the average of duplicate measurements \pm SD. p01, Cadherin-13 isoform 2; p02, Myosin-Ig MiHA HA-2 (V); p03, Beta-secretase 2 Isoform 4; p04, Amiloride-sensitive cation channel 2, neuronal isoform b; p05, granzyme H; p06, Myosin-Ig; p07, A-kinase anchor protein 3; p08, Echinoderm microtubule-associated protein-like 5; p09, Plexin-B2 precursor; p10, Exocyst complex component 1 isoform 1; p11, Myosin-Ig AC HA-2 (M). (C) T cell clone 7B5 and HA-2 control clone (5,000/well) were cocultured with HA-2^{neg} EBV-LCL IZA and HRK, untransduced or transduced with *CDH13*, at an S:R ratio of 6:1. The HA-2^{pos} EBV-LCL MRJ was included as a positive control. After overnight incubation, supernatants were harvested, and the concentration of IFN- γ was measured by ELISA. Depicted values are the average of duplicate measurements \pm SD.

Cells were washed twice and incubated with anti-PE microbeads (Miltenyi Biotec) for 15 min at 4°C. PE-labeled cells were isolated on a large separator (LS) column (Miltenyi Biotec) according to the manufacturer's instruction. Positively selected cells were stained with an anti-CD8 Alexa 700-labeled antibody (Invitrogen/Caltag) in combination with FITC-conjugated antibodies against CD4, CD14, and CD19 (BD Pharmingen). pMHC-tetramer^{pos} CD8^{pos} FITC^{neg} T cells were single-cell sorted into round-bottom 96-well plates containing 5×10^4 irradiated feeders in 100 μ L of T cell medium supplemented with 0.8 μ g/mL PHA for expansion.

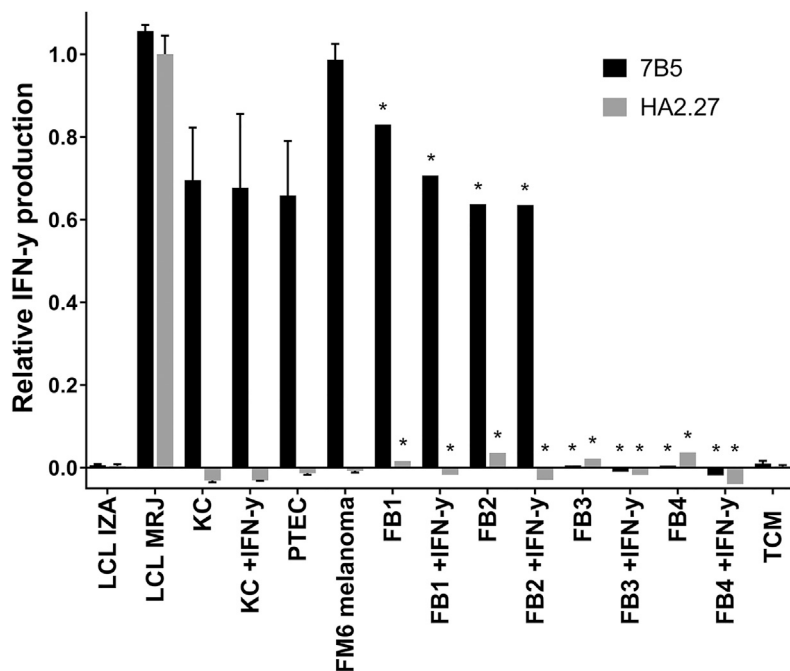
FACS Analysis

FACS acquisition was performed on an LSRII (BD Biosciences) and was analyzed using Diva Software (BD Biosciences). T cell clones were analyzed for binding to the HA-2-specific APC-labeled pMHC-tetramer, an irrelevant PE-labeled pMHC-tetramer, and an Alexa 700-conjugated antibody against CD8 (Invitrogen/Caltag). 10,000 T cells were first incubated with 2 μ g/mL pMHC-tetramers for 15 min at 37°C and washed before anti-CD8 antibodies were added and incubated for an additional 15 min at 4°C.

Functional Analysis

For analysis of IFN- γ production, 5,000 T cells were cocultured with 30,000 target cells or T2 cells loaded with peptides in 384-well plates. Peptide loading was performed by incubating T2 cells for 30 min at 37°C and 5% CO₂. T cells were washed twice before use. After overnight incubation, supernatants were harvested, and the concentration of IFN- γ was measured by ELISA (Sanquin Reagents).

To assess the peptide recognition signature, we used a previously described 9-mer CPL scan,²² consisting of 180 different peptide mixtures. In each peptide mixture all peptides have one fixed L-amino acid residue at one amino acid position, but all other positions are degenerate, enabling incorporation of any 1 of 19 natural L-amino acids in all remaining 8 positions (cysteine is excluded in



CDH13	-	-	+	+	+	+	+	+	+	+	+	+	+	-
HA-2	-	+	-	-	-	-	-	-	-	-	-	-	-	-
HLA-A*02:01	+	+	+	+	+	+	+	+	+	-	-	-	-	-

non-fixed positions). For this assay, we pulsed 20,000 T2 cells with each of the 180 different peptide mixtures at a concentration of 100 μM for 2 hr at 37°C and 5% CO₂ in 40 μL of T cell medium (IMDM supplemented with 100 IU/ml IL-2, 5% FBS, 5% human serum, 2 mM L-glutamine, and 1% penicillin/streptomycin). After peptide loading, 4,000 T cells in 20 μL of T cell medium were added per well. After overnight incubation, supernatants were harvested and IFN-γ production was measured by ELISA (Sanquin Reagents).

Analysis of the Peptide Recognition Signature

To analyze the data from the 9-mer CPL scan, we used the WSBC PI CPL webtool³⁰ that applies a mathematical strategy to match the peptide recognition signature³¹ with the human proteome to predict the most likely human self-protein-derived peptide sequences that might be recognized by the tested TCR.²⁶ We examined 100 peptides with the best log likelihood scores and removed duplicate sequences. The 10 peptide sequences that were predicted to bind HLA-A*02:01, according to NetMHC4.0, were synthesized.

Gene Transduction

The *CDH13* gene was cloned into the modified MP71-retroviral backbone, together with the truncated nerve growth factor receptor (NGF-R; also known as CD271). The constructs were transfected into Phoenix-A cells using helper vector M57 and FuGENE HD

Figure 6. The Endogenously Processed *CDH13*-Derived Peptide p01, Presented in HLA-A*02:01, Efficiently Activates the 7B5 T Cell Clone, but Not T Cell Clone HA2.27

T cell clones 7B5 and HA2.27 (5,000/well) were cocultured with different cell subsets endogenously expressing the *CDH13* gene: keratinocytes and fibroblasts, untreated or pretreated with IFN-γ for 2 days to upregulate HLA expression, proximal tubular epithelial cells, and melanoma cell line FM6. To confirm that only HLA-A*02:01-restricted epitopes are recognized, we tested the 7B5 and HA2.27 T cell clone also against HLA-A*02:01^{neg} fibroblasts, untreated or pretreated with IFN-γ. We also included the EBV-LCL controls from the patient (LCL MRJ, HLA-A*02:01^{pos} HA-2^{pos}) and donor (LCL IZA, HLA-A*02:01^{pos} HA-2^{neg}) we isolated the HA2.27 T cell clone from. After overnight incubation, supernatants were harvested, and the concentration of IFN-γ was measured by ELISA. Average IFN-γ production by the HA2.27 T cell clone stimulated with LCL MRJ was set to 1. Depicted values are the average of duplicate measurements ± SD. Asterisks (*) indicate single measurements.

reagent (Roche). Virus supernatant was harvested after 48 and 72 hr and stored at -80°C.

For transduction of EBV-LCLs, 24-well non-tissue culture plates were coated with 30 mg/mL RetroNectin (Takara) for 2 hr at room temperature and blocked with 2% human serum albumin (Sanquin Reagents) for 30 min. Viral supernatant was thawed, then 500 μL per well was added to the 24-well plate and spun down at 2,000 × g for 20 min at 4°C. 100,000 EBV-LCLs per well were added in 500 μL of fresh IMDM supplemented with 10% FBS, 2 mM L-glutamine, and 1% penicillin/streptomycin and incubated overnight at 37°C and 5% CO₂. *CDH13*^{pos} EBV-LCLs were MACS purified using anti-CD271 PE-labeled antibody (BD Pharmingen) and anti-PE microbeads (Miltenyi Biotec). *CDH13*-transduced cells were isolated on an LS column following manufacturer’s instructions.

SUPPLEMENTAL INFORMATION

Supplemental Information includes two figures and one table and can be found with this article online at <https://doi.org/10.1016/j.ymthe.2018.02.017>.

AUTHOR CONTRIBUTIONS

H.M.B. designed the experiments, performed experiments, analyzed the data, and wrote the manuscript. D.M.v.d.S. performed the 9-mer CPL scan. A.K.W. performed experiments. R.S.H. prepared the virus supernatants. L.W. provided the 9-mer CPL and reviewed and edited the manuscript. J.H.F.F reviewed and edited the manuscript. M.H.M.H. acquired the funding, supervised the research, and reviewed and edited the manuscript.

CONFLICTS OF INTEREST

The authors declare no conflict of interest.

ACKNOWLEDGMENTS

This research was supported by Landsteiner Foundation for Blood Transfusion Research grant LSBR1331. We thank Marieke Griffioen for sharing the microarray gene expression database.

REFERENCES

- Holzinger, A., Barden, M., and Abken, H. (2016). The growing world of CAR T cell trials: a systematic review. *Cancer Immunol. Immunother.* 65, 1433–1450.
- Rosenberg, S.A., and Dudley, M.E. (2009). Adoptive cell therapy for the treatment of patients with metastatic melanoma. *Curr. Opin. Immunol.* 21, 233–240.
- Besser, M.J., Shapira-Frommer, R., and Schachter, J. (2015). Tumor-infiltrating lymphocytes: clinical experience. *Cancer J.* 21, 465–469.
- Thomas, S., Stauss, H.J., and Morris, E.C. (2010). Molecular immunology lessons from therapeutic T-cell receptor gene transfer. *Immunology* 129, 170–177.
- Stromnes, I.M., Schmitt, T.M., Chapuis, A.G., Hingorani, S.R., and Greenberg, P.D. (2014). Re-adapting T cells for cancer therapy: from mouse models to clinical trials. *Immunol. Rev.* 257, 145–164.
- Robbins, P.F., Kassim, S.H., Tran, T.L., Crystal, J.S., Morgan, R.A., Feldman, S.A., Yang, J.C., Dudley, M.E., Wunderlich, J.R., Sherry, R.M., et al. (2015). A pilot trial using lymphocytes genetically engineered with an NY-ESO-1-reactive T-cell receptor: long-term follow-up and correlates with response. *Clin. Cancer Res.* 21, 1019–1027.
- Rapoport, A.P., Stadtmauer, E.A., Binder-Scholl, G.K., Goloubeva, O., Vogl, D.T., Lacey, S.F., Badros, A.Z., Garfall, A., Weiss, B., Finklestein, J., et al. (2015). NY-ESO-1-specific TCR-engineered T cells mediate sustained antigen-specific antitumor effects in myeloma. *Nat. Med.* 21, 914–921.
- Kageyama, S., Ikeda, H., Miyahara, Y., Imai, N., Ishihara, M., Saito, K., Sugino, S., Ueda, S., Ishikawa, T., Kokura, S., et al. (2015). Adoptive transfer of MAGE-A4 T-cell receptor gene-transduced lymphocytes in patients with recurrent esophageal cancer. *Clin. Cancer Res.* 21, 2268–2277.
- Johnson, L.A., Morgan, R.A., Dudley, M.E., Cassard, L., Yang, J.C., Hughes, M.S., Kammula, U.S., Royal, R.E., Sherry, R.M., Wunderlich, J.R., et al. (2009). Gene therapy with human and mouse T-cell receptors mediates cancer regression and targets normal tissues expressing cognate antigen. *Blood* 114, 535–546.
- Palmer, E. (2003). Negative selection—clearing out the bad apples from the T-cell repertoire. *Nat. Rev. Immunol.* 3, 383–391.
- Kunert, A., Obenaus, M., Lamers, C.H.J., Blankenstein, T., and Debets, R. (2017). T-cell receptors for clinical therapy: in vitro assessment of toxicity risk. *Clin. Cancer Res.* 23, 6012–6020.
- Linette, G.P., Stadtmauer, E.A., Maus, M.V., Rapoport, A.P., Levine, B.L., Emery, L., Litzky, L., Bagg, A., Carreno, B.M., Cimino, P.J., et al. (2013). Cardiovascular toxicity and titin cross-reactivity of affinity-enhanced T cells in myeloma and melanoma. *Blood* 122, 863–871.
- Stone, J.D., Harris, D.T., and Kranz, D.M. (2015). TCR affinity for p/MHC formed by tumor antigens that are self-proteins: impact on efficacy and toxicity. *Curr. Opin. Immunol.* 33, 16–22.
- Stone, J.D., and Kranz, D.M. (2013). Role of T cell receptor affinity in the efficacy and specificity of adoptive T cell therapies. *Front. Immunol.* 4, 244.
- Morgan, R.A., Chinnasamy, N., Abate-Daga, D., Gros, A., Robbins, P.F., Zheng, Z., Dudley, M.E., Feldman, S.A., Yang, J.C., Sherry, R.M., et al. (2013). Cancer regression and neurological toxicity following anti-MAGE-A3 TCR gene therapy. *J. Immunother.* 36, 133–151.
- van den Berg, J.H., Gomez-Eerland, R., van de Wiel, B., Hulshoff, L., van den Broek, D., Bins, A., et al. (2015). Case report of a fatal serious adverse event upon administration of T cells transduced with a MART-1-specific T-cell receptor. *Mol. Ther.* 23, 1541–1550.
- Raman, M.C., Rizkallah, P.J., Simmons, R., Donnellan, Z., Dukes, J., Bossi, G., Le Provost, G.S., Todorov, P., Baston, E., Hickman, E., et al. (2016). Direct molecular mimicry enables off-target cardiovascular toxicity by an enhanced affinity TCR designed for cancer immunotherapy. *Sci. Rep.* 6, 18851.
- Jahn, L., van der Steen, D.M., Hagedoorn, R.S., Hombrink, P., Kester, M.G., Schoonakker, M.P., de Ridder, D., van Veelen, P.A., Falkenburg, J.H., and Heemskerk, M.H. (2016). Generation of CD20-specific TCRs for TCR gene therapy of CD20low B-cell malignancies insusceptible to CD20-targeting antibodies. *Oncotarget* 7, 77021–77037.
- Voegt, P.J., Goulmy, E., Veenhof, W.F., Hamilton, M., Fibbe, W.E., Van Rood, J.J., and Falkenburg, J.H. (1988). Cellularly defined minor histocompatibility antigens are differentially expressed on human hematopoietic progenitor cells. *J. Exp. Med.* 168, 2337–2347.
- Goulmy, E. (1996). Human minor histocompatibility antigens. *Curr. Opin. Immunol.* 8, 75–81.
- Hickman, E.S., Lomax, M.E., and Jakobsen, B.K. (2016). Antigen selection for enhanced affinity T-cell receptor-based cancer therapies. *J. Biomol. Screen.* 21, 769–785.
- Wooldridge, L., Laugel, B., Ekeruche, J., Clement, M., van den Berg, H.A., Price, D.A., and Sewell, A.K. (2010). CD8 controls T cell cross-reactivity. *J. Immunol.* 185, 4625–4632.
- Heemskerk, M.H., Hoogeboom, M., de Paus, R.A., Kester, M.G., van der Hoorn, M.A., Goulmy, E., Willemze, R., and Falkenburg, J.H. (2003). Redirection of antileukemic reactivity of peripheral T lymphocytes using gene transfer of minor histocompatibility antigen HA-2-specific T-cell receptor complexes expressing a conserved alpha joining region. *Blood* 102, 3530–3540.
- Marijt, W.A., Heemskerk, M.H., Kloosterboer, F.M., Goulmy, E., Kester, M.G., van der Hoorn, M.A., van Luxemburg-Heys, S.A., Hoogeboom, M., Mutis, T., Drijfhout, J.W., et al. (2003). Hematopoiesis-restricted minor histocompatibility antigens HA-1- or HA-2-specific T cells can induce complete remissions of relapsed leukemia. *Proc. Natl. Acad. Sci. USA* 100, 2742–2747.
- Pont, M.J., Honders, M.W., Kremer, A.N., van Kooten, C., Out, C., Hiemstra, P.S., de Boer, H.C., Jager, M.J., Schmelzer, E., Vries, R.G., et al. (2016). Microarray gene expression analysis to evaluate cell type specific expression of targets relevant for immunotherapy of hematological malignancies. *PLoS ONE* 11, e0155165.
- Wooldridge, L., Ekeruche-Makinde, J., van den Berg, H.A., Skowera, A., Miles, J.J., Tan, M.P., Dolton, G., Clement, M., Llewellyn-Lacey, S., Price, D.A., et al. (2012). A single autoimmune T cell receptor recognizes more than a million different peptides. *J. Biol. Chem.* 287, 1168–1177.
- Degaque, N., Brouard, S., and Souillou, J.P. (2016). Cross-reactivity of TCR repertoire: current concepts, challenges, and implication for allotransplantation. *Front. Immunol.* 7, 89.
- Singh, N.K., Riley, T.P., Baker, S.C.B., Borrman, T., Weng, Z., and Baker, B.M. (2017). Emerging concepts in TCR specificity: rationalizing and (maybe) predicting outcomes. *J. Immunol.* 199, 2203–2213.
- Di Stasi, A., Tey, S.K., Dotti, G., Fujita, Y., Kennedy-Nasser, A., Martinez, C., Straathof, K., Liu, E., Duret, A.G., Grilley, B., et al. (2011). Inducible apoptosis as a safety switch for adoptive cell therapy. *N. Engl. J. Med.* 365, 1673–1683.
- Szomolay, B., Liu, J., Brown, P.E., Miles, J.J., Clement, M., Llewellyn-Lacey, S., Dolton, G., Ekeruche-Makinde, J., Lissina, A., Schauenburg, A.J., et al. (2016). Identification of human viral protein-derived ligands recognized by individual MHCI-restricted T-cell receptors. *Immunol. Cell Biol.* 94, 573–582.
- Wooldridge, L. (2013). Individual MHCI-restricted T-cell receptors are characterized by a unique peptide recognition signature. *Front. Immunol.* 4, 199.

YMTHE, Volume 26

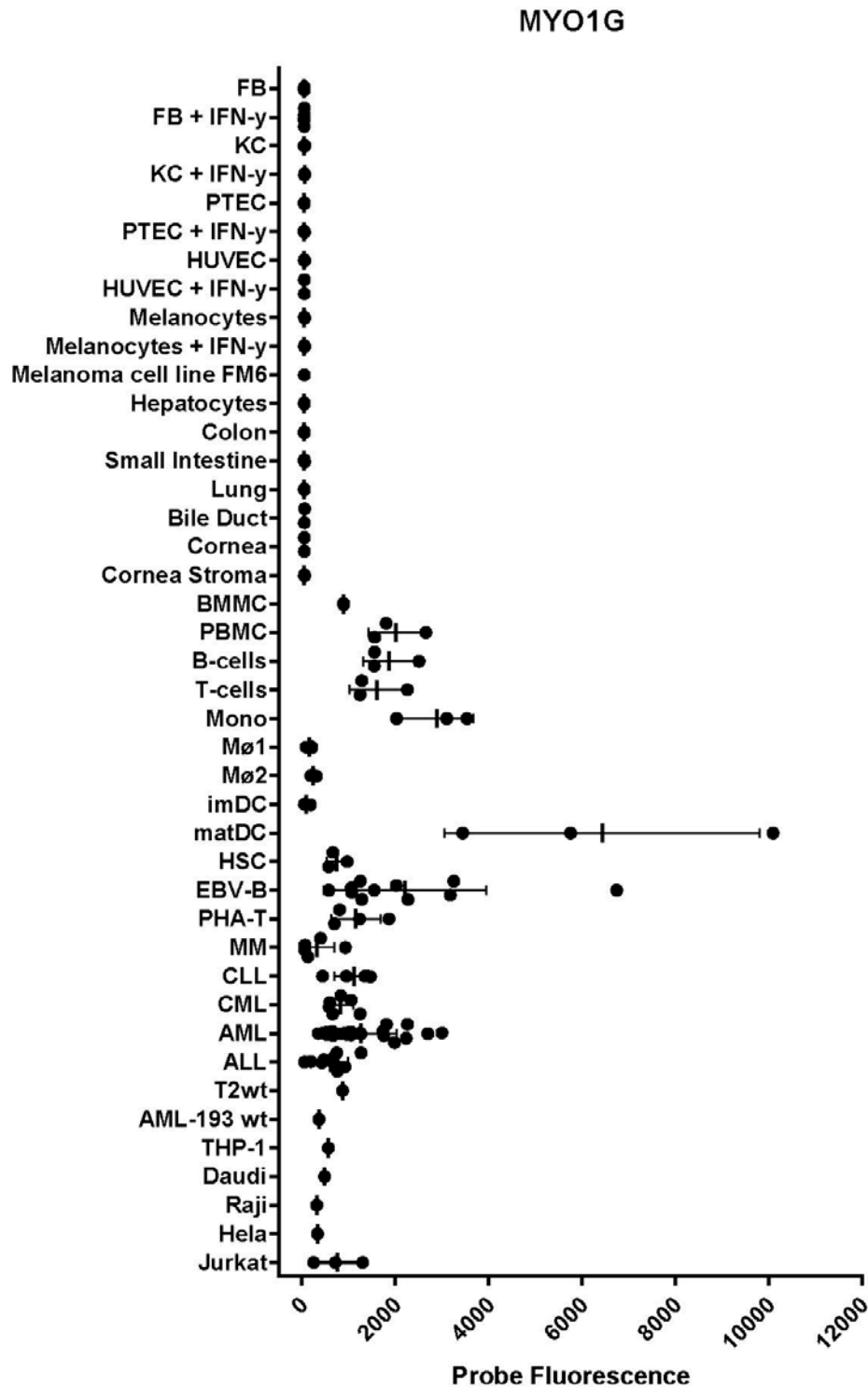
Supplemental Information

Preclinical Strategies to Identify Off-Target

Toxicity of High-Affinity TCRs

Helena M. Bijen, Dirk M. van der Steen, Renate S. Hagedoorn, Anne K. Wouters, Linda Wooldridge, J.H. Frederik Falkenburg, and Mirjam H.M. Heemskerk

Supplementary Figure 1: Gene expression profile for minor histocompatibility antigen HA-2 (MYO1G). Probe fluorescence intensity is shown on the x-axis in logarithmic scale. On the y-axis malignant and healthy (non-)hematopoietic cell types are shown. Each dot represents a different sample and the mean and standard deviation of gene expression is shown for each cell type.



Supplementary Table 1: Potential cross-reactive human self-protein derived peptide targets of the 7B5 T-cell clone. The peptides in this table are selected based on their predicted recognition by the 7B5 T-cell clone according to a CPL-driven search of the human self-protein database conducted using the WSBC PI CPL webtool.

Output score	Peptide	Protein
-16,869723	NVGEVYGVV	gi 34577063 ref NP_001117.2 adenylosuccinate synthetase isozyme 2
-16,869723	NVGEVYGVV	ADENYLOSUCCINATE SYNTHETASE ISOZYME 2 HOMO SAPIENS
-16,930872	SVGSVLLTV	gi 333944015 ref NP_001207417.1 cadherin-13 isoform 2
-16,930872	SVGSVLLTV	gi 4502719 ref NP_001248.1 cadherin-13 isoform 1 preproprotein
-16,930872	SVGSVLLTV	gi 333944018 ref NP_001207418.1 cadherin-13 isoform 3 precursor
-16,930872	SVGSVLLTV	gi 333944020 ref NP_001207419.1 cadherin-13 isoform 4
-17,220057	SVGEVIEVL	gi 7662482 ref NP_055723.1 dolichol kinase
-17,281433	YIGEVLSV	gi 239582755 ref NP_149043.2 myosin-Ig
-17,281433	YIGEVLSV	sp B0I1T2-4 MYO1G_HUMAN Isoform 4 of Unconventional myosin-Ig OS=Homo sapiens GN=MYO1G
-17,281433	YIGEVLSV	sp B0I1T2-2 MYO1G_HUMAN Isoform 2 of Unconventional myosin-Ig OS=Homo sapiens GN=MYO1G
-17,281433	YIGEVLSV	sp B0I1T2-3 MYO1G_HUMAN Isoform 3 of Unconventional myosin-Ig OS=Homo sapiens GN=MYO1G
-17,353998	TVGELLVTI	gi 156938343 ref NP_055874.2 talin-2
-17,374766	NSGEVIVTL	gi 41393559 ref NP_904325.2 kinesin-like protein KIF1B isoform alpha
-17,374766	NSGEVIVTL	gi 41393563 ref NP_055889.2 kinesin-like protein KIF1B isoform b
-17,374766	NSGEVIVTL	Kinesin-like protein KIF1B Homo sapiens
-17,374766	NSGEVIVTL	sp O60333-4 KIF1B_HUMAN Isoform 4 of Kinesin-like protein KIF1B OS=Homo sapiens GN=KIF1B
-17,374766	NSGEVIVTL	sp O60333 KIF1B_HUMAN Kinesin-like protein KIF1B OS=Homo sapiens GN=KIF1B PE=1 SV=5
-17,392979	LVGFVLLTV	gi 22749415 ref NP_689926.1 dolichyl-diphosphooligosaccharide--protein glycosyltransferase subunit STT3A
-17,501319	WGGEVLIVA	gi 156564359 ref NP_212134.3 riboflavin transporter 2
-17,795412	GVGEVLHVK	gi 209954788 ref NP_001129625.1 cyclic AMP-dependent transcription factor ATF-6 beta isoform b
-17,795412	GVGEVLHVK	gi 20631977 ref NP_004372.3 cyclic AMP-dependent transcription factor ATF-6 beta isoform a
-17,821511	TTGEVVVTM	gi 35493860 ref NP_919304.1 otoferlin isoform d
-17,821511	TTGEVVVTM	gi 35493868 ref NP_004793.2 otoferlin isoform b
-17,840203	SGGEVIFTK	sp Q9Y334-2 VWA7_HUMAN Isoform 2 of von Willebrand factor A domain-containing protein 7 OS=Homo sapiens GN=VWA7
-17,840203	SGGEVIFTK	gi 153945852 ref NP_079534.2 protein G7c precursor
-17,891018	KVGEVIVTK	gi 41399285 ref NP_955472.1 60 kDa heat shock protein, mitochondrial
-17,898825	FVGEDLVTI	sp Q9Y5Z0-4 BACE2_HUMAN Isoform 4 of Beta-secretase 2 OS=Homo sapiens GN=BACE2
-17,898825	FVGEDLVTI	gi 21040360 ref NP_620476.1 beta-secretase 2 isoform C preproprotein
-17,898825	FVGEDLVTI	Beta-secretase 2 Homo sapiens
-17,898825	FVGEDLVTI	gi 21040362 ref NP_620477.1 beta-secretase 2 isoform B preproprotein
-17,898825	FVGEDLVTI	sp Q9Y5Z0-5 BACE2_HUMAN Isoform 5 of Beta-secretase 2 OS=Homo sapiens GN=BACE2
-17,898825	FVGEDLVTI	gi 19923395 ref NP_036237.2 beta-secretase 2 isoform A preproprotein
-17,901998	STGEVVVTM	sp Q9HC10-5 OTOF_HUMAN Isoform 5 of Otoferlin OS=Homo sapiens GN=OTOF
-17,901998	STGEVVVTM	gi 34740331 ref NP_919224.1 otoferlin isoform a
-17,901998	STGEVVVTM	gi 35493853 ref NP_919303.1 otoferlin isoform c
-17,913793	AFGEVAVVK	Serine/threonine-protein kinase MRCK beta Homo sapiens
-17,913793	AFGEVAVVK	sp Q5VT25-4 MRCKA_HUMAN Isoform 4 of Serine/threonine-protein kinase MRCK alpha OS=Homo sapiens GN=CDC42BP7

-17,913793	AFGEVAVVK	sp Q5VT25 MRCKA_HUMAN Serine/threonine-protein kinase MRCK alpha OS=Homo sapiens GN=CDC42BPA PE=1 SV=1
-17,913793	AFGEVAVVK	CDC42BPB protein Homo sapiens
-17,913793	AFGEVAVVK	gi 30089962 ref NP_003598.2 serine/threonine-protein kinase MRCK alpha isoform B
-17,913793	AFGEVAVVK	gi 115527097 ref NP_006026.3 serine/threonine-protein kinase MRCK beta
-17,913793	AFGEVAVVK	gi 30089960 ref NP_055641.3 serine/threonine-protein kinase MRCK alpha isoform A
-17,913793	AFGEVAVVK	sp Q5VT25-6 MRCKA_HUMAN Isoform 6 of Serine/threonine-protein kinase MRCK alpha OS=Homo sapiens GN=CDC42BPA
-17,913793	AFGEVAVVK	sp Q5VT25-2 MRCKA_HUMAN Isoform 2 of Serine/threonine-protein kinase MRCK alpha OS=Homo sapiens GN=CDC42BPA
-17,935032	TVGEVFYTK	gi 295842556 ref NP_001171516.1 choline transporter-like protein 4 isoform 3
-17,935032	TVGEVFYTK	gi 148612887 ref NP_079533.2 choline transporter-like protein 4 isoform 1
-18,093028	ANGEVLCTV	gi 260654089 ref NP_940972.2 brorin precursor
-18,094741	YIGENILVL	gi 21536349 ref NP_001086.2 amiloride-sensitive cation channel 2, neuronal isoform b
-18,094741	YIGENILVL	gi 21536351 ref NP_064423.2 amiloride-sensitive cation channel 2, neuronal isoform a
-18,145863	SGGESLLVK	gi 89886477 ref NP_037535.2 striatin-4 isoform 1
-18,145863	SGGESLLVK	gi 89886480 ref NP_001034966.1 striatin-4 isoform 2
-18,15759	TFGEVLMVQ	gi 6678271 ref NP_031401.1 TAR DNA-binding protein 43
-18,15759	TFGEVLMVQ	sp Q13148-2 TADBP_HUMAN Isoform 2 of TAR DNA-binding protein 43 OS=Homo sapiens GN=TARDBP
-18,15759	TFGEVLMVQ	TAR DNA-binding protein-43 Homo sapiens
-18,167442	SVGEILDVI	gi 194272140 ref NP_055901.2 dendrin
-18,304123	TIGEIQVTL	gi 148596984 ref NP_004478.3 Golgin subfamily B member 1
-18,311744	DIGEVLVVG	gi 24234688 ref NP_004125.3 stress-70 protein, mitochondrial precursor
-18,318139	TLQEVLTV	Granzyme H Homo sapiens
-18,318139	TLQEVLTV	gi 15529990 ref NP_219491.1 granzyme H precursor
-18,325342	SKGEVLSVL	gi 13540565 ref NP_110415.1 transmembrane 7 superfamily member 4
-18,334446	SEEEVLTV	gi 13787217 ref NP_001438.1 protocadherin Fat 2 precursor
-18,344272	SAGELLTL	gi 194595501 ref NP_689716.4 uncharacterized protein C20orf132 isoform 1
-18,344272	SAGELLTL	gi 47578111 ref NP_998796.1 uncharacterized protein C20orf132 isoform 2
-18,344272	SAGELLTL	gi 47578113 ref NP_998797.1 uncharacterized protein C20orf132 isoform 3
-18,344272	SAGELLTL	sp Q9H579 CT132_HUMAN Uncharacterized protein C20orf132 OS=Homo sapiens GN=C20orf132 PE=2 SV=2
-18,345617	QEGEVEIVV	sp Q8NDH2 CC168_HUMAN Coiled-coil domain-containing protein 168 OS=Homo sapiens GN=CCDC168 PE=2 SV=2
-18,345617	QEGEVEIVV	gi 226246554 ref NP_001139669.1 coiled-coil domain-containing protein 168
-18,356731	LGGFVLLVV	>gi 42822882 ref NP_981947.1 fat storage-inducing transmembrane protein 1
-18,361006	NMGEVLLVR	gi 31711992 ref NP_001922.2 dihydrolipoyllysine-residue acetyltransferase component of pyruvate dehydrogenase complex, mitochondrial precursor
-18,361006	NMGEVLLVR	Dihydrolipoyllysine-residue acetyltransferase Homo sapiens
-18,393409	FIGEVVSV	gi 51100974 ref NP_056009.1 myosin-Id
-18,400716	SCGEVIHVK	sp Q9H2U2-2 IPYR2_HUMAN Isoform 2 of Inorganic pyrophosphatase 2, mitochondrial OS=Homo sapiens GN=PPA2
-18,400716	SCGEVIHVK	gi 77812678 ref NP_008834.3 inorganic pyrophosphatase 2, mitochondrial isoform 2 precursor
-18,400716	SCGEVIHVK	gi 77812680 ref NP_789842.2 inorganic pyrophosphatase 2, mitochondrial isoform 3 precursor
-18,400716	SCGEVIHVK	gi 29171702 ref NP_789845.1 inorganic pyrophosphatase 2, mitochondrial isoform 1 precursor
-18,405009	TVGIVIVV	gi 7662320 ref NP_055628.1 leucine-rich repeats and immunoglobulin-like domains protein 2 precursor
-18,453565	SVGEVLQSV	gi 21493041 ref NP_006413.2 A-kinase anchor protein 3
-18,465921	SAGEVLMTI	gi 31317272 ref NP_055806.2 WD repeat and FYVE domain-containing protein 3
-18,465921	SAGEVLMTI	sp Q8IZQ1-2 WDFY3_HUMAN Isoform 2 of WD repeat and FYVE domain-containing protein 3 OS=Homo sapiens GN=WDFY3

-18,466015	SPGEVLRTL	gi 93102424 ref NP_055906.2 protein FAM179B
-18,466015	SPGEVLRTL	sp Q9Y4F4-3 F179B_HUMAN Isoform 3 of Protein FAM179B OS=Homo sapiens GN=FAM179B
-18,466015	SPGEVLRTL	sp Q9Y4F4-2 F179B_HUMAN Isoform 2 of Protein FAM179B OS=Homo sapiens GN=FAM179B
-18,470252	YIGQVLVTA	gi 34485720 ref NP_899243.1 echinoderm microtubule-associated protein-like 5
-18,470252	YIGQVLVTA	sp Q05BV3-4 EMAL5_HUMAN Isoform 4 of Echinoderm microtubule-associated protein-like 5 OS=Homo sapiens GN=EML5
-18,470252	YIGQVLVTA	sp Q05BV3-2 EMAL5_HUMAN Isoform 2 of Echinoderm microtubule-associated protein-like 5 OS=Homo sapiens GN=EML5
-18,470252	YIGQVLVTA	sp Q05BV3 EMAL5_HUMAN Echinoderm microtubule-associated protein-like 5 OS=Homo sapiens GN=EML5 PE=2 SV=3
-18,472182	AQGEVQLTV	gi 149363636 ref NP_036533.2 plexin-B2 precursor
-18,478842	ADGEVDVVV	Amiloride-sensitive amine oxidase Homo sapiens
-18,478842	ADGEVDVVV	Diamine oxidase Homo sapiens
-18,478842	ADGEVDVVV	sp P19801-2 ABP1_HUMAN Isoform 2 of Amiloride-sensitive amine oxidase [copper-containing] OS=Homo sapiens GN=ABP1
-18,478842	ADGEVDVVV	gi 73486661 ref NP_001082.2 amiloride-sensitive amine oxidase [copper-containing] precursor
-18,486044	NGGELFLTV	gi 4505351 ref NP_001534.1 bifunctional heparan sulfate N-deacetylase/N-sulfotransferase 1
-18,486044	NGGELFLTV	sp P52848-2 NDST1_HUMAN Isoform 2 of Bifunctional heparan sulfate N-deacetylase/N-sulfotransferase 1 OS=Homo sapiens GN=NDST1
-18,495633	TLGNVLVTV	gi 67944634 ref NP_001020095.1 exocyst complex component 1 isoform 1
-18,495633	TLGNVLVTV	gi 30410716 ref NP_839955.1 exocyst complex component 1 isoform 2
-18,503243	FVGFVIVTF	sp Q13936-34 CAC1C_HUMAN Isoform 34 of Voltage-dependent L-type calcium channel subunit alpha-1C OS=Homo sapiens GN=CACNA1C
-18,503243	FVGFVIVTF	sp Q13936-18 CAC1C_HUMAN Isoform 18 of Voltage-dependent L-type calcium channel subunit alpha-1C OS=Homo sapiens GN=CACNA1C
-18,503243	FVGFVIVTF	sp Q13936-28 CAC1C_HUMAN Isoform 28 of Voltage-dependent L-type calcium channel subunit alpha-1C OS=Homo sapiens GN=CACNA1C
-18,503243	FVGFVIVTF	gi 192807298 ref NP_001122311.1 voltage-dependent L-type calcium channel subunit alpha-1D isoform c
-18,503243	FVGFVIVTF	sp Q13936-17 CAC1C_HUMAN Isoform 17 of Voltage-dependent L-type calcium channel subunit alpha-1C OS=Homo sapiens GN=CACNA1C

Supplementary Figure 2: Gene expression profile for *CDH13*. Probe fluorescence intensity is shown on the x-axis in logarithmic scale. On the y-axis malignant and healthy (non-) hematopoietic cell types are shown. Each dot represents a different sample and the mean and standard deviation of gene expression is shown for each cell type.

